

Research Article

Reduced Graphene Oxide Decorated with Cu Nanoparticles as an Efficient Catalyst for Ullmann-Type *N*-Arylation Reactions

Sodeh Sadjadi^{id}

Radiation Application Research School, Nuclear Science and Technology Research Institute, P.O. Box 11365-3486, Tehran, Iran
E-mail: sdsadjadi@aeoi.org.ir

Received: 18 September 2024; **Revised:** 24 October 2024; **Accepted:** 24 October 2024

Abstract: Ullmann-type aryl amination of aryl halides catalyzed by reduced graphene oxide decorated with copper nanoparticles was investigated. The reduced graphene oxide-supported copper nanoparticles were prepared via simultaneous electrodeposition of copper nanoparticles and reduction of graphene oxide by a facile cyclic voltammetry method in the absence of any reducing agent or volatile solvents. The proposed method is simple, general, ligand-free, and efficient to afford *N*-arylated compounds in high yield. The hot filtration test suggests the present reaction would proceed via heterogeneous nature. The catalyst showed high stability and could easily be recovered and reused without any considerable loss of its catalytic activity.

Keywords: reduced graphene oxide, copper nanoparticles, aryl halides, amines, ullmann C–N coupling

1. Introduction

Ullmann-type aryl amination has been extensively employed in both academia and industry because of its potential applications for the development of pharmaceuticals, polymers, and functional materials^{1–3}. Recently, the synthetic scope of this reaction has grown when significant progresses in the development of mild reaction conditions and new catalytic systems have been made to reduce the environmental impact of this process (the classical Ullmann reaction relied upon stoichiometric copper reagent, which on scale-up leads to the problem of waste disposal)^{4,5}. In particular, palladium complexes^{6–10} with various ligands and modified Cu-catalyzed coupling systems with many Cu(I) and Cu(II) derivatives^{11–18} have been studied for Ullmann C–N coupling. Compared to the Pd-catalyzed method, which required air- and moisture-sensitive conditions and higher cost, Cu-catalyzed coupling systems have been receiving more attention due to their lower toxicity and costs of Cu and the relative ligands^{19,20}. However, most catalysts that accelerate Ullmann amination rely on specific ligands and are typically used under homogeneous conditions, which hampers their recyclability and practical applicability²¹. Among the various copper-based catalysts, ligand-free heterogeneous zero-valent copper nanoparticles (Cu NPs) continue to attract considerable and increasing researchers' attention owing to the advantages of high specific surface area and size and shape-tunable catalytic properties. However, the wide application of Cu NPs is restricted by the challenges of overcoming the catalyst separation and deactivation by self-aggregation, in addition to Cu's inherent instability and surface oxidation²². In this sense, catalytic systems that rely on composites with active metallic centers may be good alternatives to overcome the problems mentioned earlier. Various types of copper composites have

been under intensive studies and revealed a promising role in a wide range of catalytic reactions, including Ullmann C–N coupling^{23,24}.

Recent advances in the catalytic systems based on metal-embedded carbon networks have led to the development of various carbon-based Cu NPs composites²². Graphene oxide (GO), a sp²-hybridized carbon-based material with a hexagonal monolayer network, has gained a growing interest in catalysis due to its significant characteristics such as large surface area, thermal stability, high stability in acidic and basic conditions, minimal mass-transfer limitations, electronic transfer property, low cost, and reduced negative impacts on the environment^{25–27}. However, the surface oxygen-containing functional groups cause the high dispersibility of GO in aqueous phases, which is an obstacle for separating and recycling of the graphene-based catalysts²⁸. GO also has defective sites in the basal plane due to the high content of oxygen surface groups, which causes the losses in catalytic activity²⁶. Moreover, GO suffers from a severe tendency to form tightly packed structure due to the strong π - π interaction between neighboring sheets, resulting in the reduced absorptivity²⁸. Reduction of GO using chemical, electrochemical, or thermal methods can repair the defects in GO by removing oxygen-containing functional groups and restoring the conjugated network.

In the present paper a simple electrochemical route to prepare the composite of reduced graphene oxide (rGO) decorated with Cu NPs is reported and its catalytic activity in Ullmann C–N coupling is tested. It is demonstrated that the one-pot electrodeposition is a low-temperature operation, simple, and cost-effective method to prepare both Cu NPs and rGO without using any reducing agent or volatile solvents and could incorporate nanoparticles homogeneously throughout the rGO matrix. The efficient and recyclable Cu-rGO catalyst successfully demonstrated its ability to construct *N*-arylated compounds via Ullmann coupling under ligand-free conditions at relatively mild conditions.

2. Results and discussion

2.1 Catalyst synthesis and characterization

In this paper, a simple one-step electrodeposition method to fabricate a novel Cu-rGO nanocomposite was proposed in which, the reduction of Cu(II) salt and GO is carried out simultaneously, generating a hydrophobic copper-based catalyst. As compared to the previous work, the electrochemical deposition route possesses the advantage of the preparation of Cu-rGO nanocomposite without using toxic reducing agents such as NaBH₄ and hydrazine hydrate or volatile solvents^{29,30}.

The morphological characterization of the Cu-rGO was performed by field emission scanning electron microscope (FE-SEM). In compare with the bare electrode (Figure S1a), the rGO-modified electrode surface is covered by the crumpled and wrinkled rGO nanosheet (Figure S1b). The morphology of Cu-rGO-modified electrode has obvious change as compared with that of the rGO-modified electrode as depicted in Figure S1c and the existence of Cu particles can be clearly observed. The size distribution of the Cu NPs on the rGO nanosheets obtained by Image J software (Figure S1d) showed the average particle size around 25 nm in diameter.

The XRD pattern of the Cu-rGO catalyst along with the diffraction patterns of Cu and rGO are depicted in Figure S2. The XRD pattern of the Cu-rGO shows all the characteristic peaks of the Cu with an additional broad peak due to the presence of rGO. The absence of the characteristic peak of GO at $2\theta \sim 11.06^\circ$ corresponding to the (001) plane and a broad diffraction peak at $2\theta \sim 23^\circ$ suggest that graphene oxide was successfully reduced to rGO. The distinctive peaks centered at $2\theta \sim 43.3, 50.5, 74.2, 90.0,$ and 95.10° can be ascribed to the (111), (200), (220), (311), and (222) facets of the face-centered cubic structures of Cu crystal, respectively (JCPDS card no. 4-836).

FT-IR spectrum of Cu-rGO (Figure S3) represents characteristic absorption bands at 3379, 2927–2877, 1710, and 1519 cm⁻¹ arising due to the stretching vibrations of O–H, C–H, C=O, and C=C functionalities, respectively. In addition, other adsorption bands found at 1143 cm⁻¹ and 1033 cm⁻¹ could correspond to the stretching vibrations of epoxy (C–O) and alkoxy (C–O) groups³¹.

Thermogravimetric analysis (TGA) was performed to study the thermal stability of the Cu-rGO nanocomposite. The TGA thermogram of Cu-rGO (Figure S4) shows a thermal degradation started below 100 °C with a major loss of weight at around 150 °C, that accounts for mass loss of ~18%, which is arising from the loss of residual water adsorbed on the

Cu-rGO and pyrolysis of oxygen-containing functional groups. The second weight loss (~32%) at around 450 to 530 °C can be ascribed to the degradation of the C–C skeleton of rGO.

2.2 Optimization of reaction conditions

In order to investigate the optimum reaction conditions, diphenylamine formation from aniline and iodobenzene was surveyed as a model reaction. The initial experiments were conducted by running the model reaction in the presence of Cs₂CO₃ and 3 mol% of Cu-rGO catalyst in DMF for 6 h at 110 °C under air. This reaction afforded diphenylamine in 93% yield with almost complete selectivity. *N*-arylation of aniline did not happen without the Cu-rGO catalyst or using bare rGO, which signified that copper is the active site for the Ullmann C–N coupling. Much lower yields were achieved at lower amounts of catalyst (1 and 2 mol%) under the same reaction conditions, whereas the product's yield did not change significantly when the amount of catalyst was increased from 3 mol% to 4 mol%. Among the solvents screened, DMSO, NMP, acetonitrile, toluene, dioxane, and DMF, the former was found to be the best concerning the yield of diphenylamine. The results demonstrated that the presence of a base in the reaction mixture was necessary, and Cs₂CO₃ was the most effective in comparison to other bases, such as K₃PO₄, K₂CO₃, KOH, and Et₃N. The reaction afforded the coupling product in lower yields when the reaction time was shortened to 2 h and 4 h. The results revealed that the temperature has a key role in the progress of the reaction. A higher temperature (110 °C) allowed a better product yield.

Table 1. Optimization of the reaction conditions for the Ullmann coupling of iodobenzene and aniline^a

Entry	Catalyst Type	Catalyst Amount (mol%)	Solvent	Base	Temp. (°C)	Time (h)	Yield (%) ^b
1	No catalyst	-	DMF	Cs ₂ CO ₃	110	6	0
2	rGO	-	DMF	Cs ₂ CO ₃	110	6	0
3	Cu-rGO	3	DMF	Cs ₂ CO ₃	110	6	93
4	Cu-rGO	2	DMF	Cs ₂ CO ₃	110	6	81
5	Cu-rGO	1	DMF	Cs ₂ CO ₃	110	6	69
6	Cu-rGO	4	DMF	Cs ₂ CO ₃	110	6	95
7	Cu-rGO	3	DMSO	Cs ₂ CO ₃	110	6	70
8	Cu-rGO	3	NMP	Cs ₂ CO ₃	110	6	61
9	Cu-rGO	3	acetonitrile	Cs ₂ CO ₃	110	6	52
10	Cu-rGO	3	toluene	Cs ₂ CO ₃	110	6	25
11	Cu-rGO	3	dioxane	Cs ₂ CO ₃	110	6	38
12	Cu-rGO	3	DMF	-	110	6	0
13	Cu-rGO	3	DMF	K ₃ PO ₄	110	6	63
14	Cu-rGO	3	DMF	K ₂ CO ₃	110	6	75
15	Cu-rGO	3	DMF	KOH	110	6	58
16	Cu-rGO	3	DMF	Et ₃ N	110	6	16
17	Cu-rGO	3	DMF	Cs ₂ CO ₃	110	2	56
18	Cu-rGO	3	DMF	Cs ₂ CO ₃	110	4	75
19	Cu-rGO	3	DMF	Cs ₂ CO ₃	90	6	21
20	Cu-rGO	3	DMF	Cs ₂ CO ₃	70	6	Trace

^a Reaction conditions: iodobenzene (5 mmol), aniline (7.5 mmol), catalyst, solvent (2.5 mL), base (10 mmol) were stirred at appropriate time and temperature. ^b Isolated yield.

2.3 Synthetic scope

With the optimized conditions in hand, the general applicability of this reaction system was explored with a series of substrates, and the results are summarized in Table 2. The present catalytic system worked well for the coupling of arylamines bearing electron-donating (entries 1–4, Table 2) and electron-withdrawing groups (entries 5–6, Table 2) with iodobenzene, leading to diarylamines with good to high yield and selectivity (>99%). The results revealed that electronic effects in the arylamine influence the reaction rate. As illustrated in Table 2, arylamines possessing electron-donating groups (entries 1–4, Table 2) produced the corresponding diarylamines more quickly in comparison to arylamines having electron-withdrawing groups (entries 5–6, Table 2). As expected, presence of the electron-donating group at *meta*-position of the arylamine gave the coupling product in lower yield compared to the corresponding *para*-substituted arylamine (entries 4 and 3, Table 2). The *ortho*-substituted arylamine (entry 2, Table 2) had a little lower yield but with a complete selectivity probably due to the effect of steric hindrance of the substituent. Various heterocyclic amines could also furnish

the corresponding *N*-arylated products with high yields and selectivity under standard conditions (entries 7 and 8, Table 2). The catalytic efficiency of Cu-rGO in the *N*-arylation of aniline with various substituted iodobenzene was next explored (entries 9 and 10, Table 2). The electronic nature of the substituent in the iodobenzene showed a pronounced affect in the reaction rate and the products' yield. Iodobenzene bearing electron-donating substituent (entries 9, Table 2) showed less reactivity even after longer reaction times than that with electron-withdrawing substituent (entries 10, Table 2). Under these reaction conditions the cross-coupling of aniline with bromobenzene (entries 11, Table 2) produced the corresponding *N*-arylamine in moderate yield. However, good yield was obtained by carrying out the reaction at a higher temperature (entry 11, Table 2). Using chlorobenzene as a substrate, only a small amount of diarylamine was detected even after heating at 140 °C and prolonged reaction time (entry 12, Table 2).

Table 2. Ullmann *N*-arylation reaction of amines with arylhalides^a

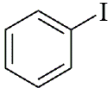
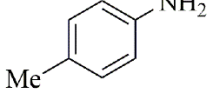
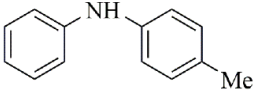
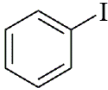
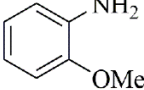
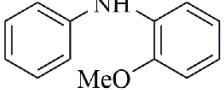
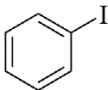
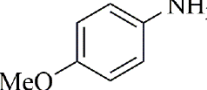
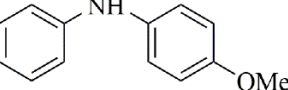
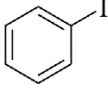
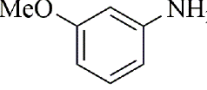
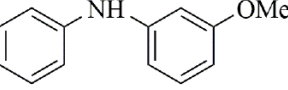
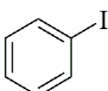
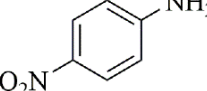
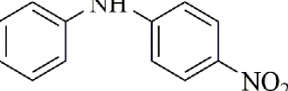
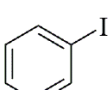
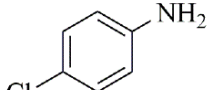
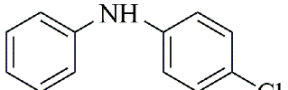
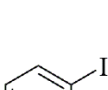
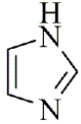
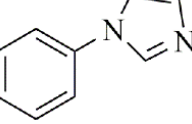
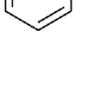
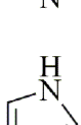
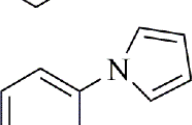
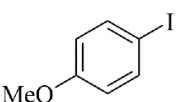
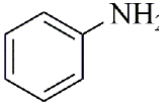
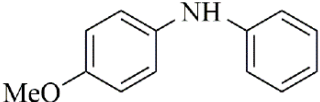
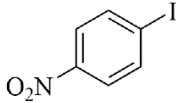
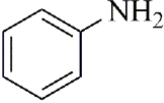
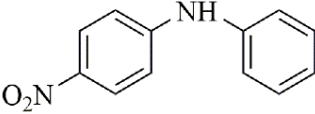
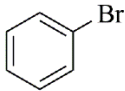
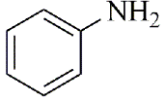
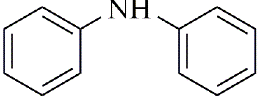
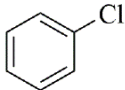
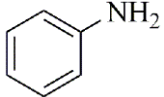
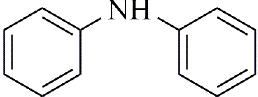
Entry	Aryl Halides	Amines	Products	Time (h)	Yield (%) ^b
1				6	91
2				7	84
3				6	89
4				7	81
5				8	78
6				8	80
7				6	93
8				6	85
9				8	75

Table 2. Cont.

Entry	Aryl Halides	Amines	Products	Time (h)	Yield (%) ^b
10				6	80
11 ^c				9	68
12 ^c				12	34

^a Reaction conditions: arylhalide (5 mmol), amine (7.5 mmol), catalyst, solvent (2.5 mL), Cs₂CO₃ (10 mmol) were stirred at 110 °C and appropriate time. ^b Isolated yield (confirmed by GC, purity ≥ 98%). ^c reaction was carried out at 140 °C.

2.4 Heterogeneity and reusability

The recyclability of the Cu-rGO catalyst was also explored for the *N*-arylation of the model reaction. The catalyst could be recycled and reused for up to three consecutive cycles under similar conditions. To demonstrate the recyclability of the Cu-rGO catalyst, X-ray diffraction analysis of the recovered catalyst was studied and compared with fresh Cu-rGO. The XRD pattern of the recovered catalyst was similar to that of fresh Cu-rGO, confirming the stability of the Cu-rGO structure upon recycling.

In order to prove the heterogeneous nature of the catalyst the hot filtration test was conducted. According to the results, the *N*-arylation reaction did not proceed in the absence of the catalyst, confirming Cu-rGO was a heterogeneous catalyst.

3. Experimental

3.1 Preparation of Cu-rGO catalyst

GO was synthesized by a modified Hummers' method and the detailed process operations were described in the previous work²⁸. The electrodeposition of Cu NPs and rGO was performed simultaneously by cyclic voltammetry (CV) method. The cyclic voltammeteries were carried out in a conventional airtight three-electrode cell containing 5 mL of GO (0.1 mg mL⁻¹) and 5 mL of 0.01 M CuSO₄ at room temperature. The working electrode was a stainless-steel electrode and the auxiliary and reference electrodes were a Pt wire and an Ag/AgCl electrode (KCl, 3 M), respectively. Five consecutive CVs (sweep rate 20 mVs⁻¹) were carried out in the potential range 0.0 to -1.5 V with N₂ bubbling.

For comparison, reduced graphene was prepared by the electrodeposition under the same conditions without adding CuSO₄.

3.2 Catalytic reaction

A mixture of aryl halide (5 mmol), amine (7.5 mmol), base (10 mmol), and Cu-rGO (3 mol% for Cu) in 5 mL of solvent was heated at the indicated temperature and stirred for the specified time in Table 1. After completion of the reaction (monitored by TLC), the cooled mixture was diluted with ethyl acetate (5 mL), and the catalyst was removed by centrifugal separation and washed several times with ethyl acetate. The filtrate was poured into water and the product extracted with ethyl acetate (3 × 10 mL). The combined organic fraction was dried over Na₂SO₄ and subjected to solvent evaporation under vacuum. The residue was purified by chromatography using silica gel eluting with an appropriate hexane/ethyl acetate mixture to afford the corresponding *N*-arylamines in pure forms.

3.3 Hot filtration test

The hot filtration test is applied by filtering off Cu-rGO catalyst from the hot reaction mixture after 3 h. The filtrate was monitored by GC to obtain conversion of aniline. *N*-arylation reaction in the filtrate was continued for 3 h and the aniline conversion was detected by GC again.

3.4 Characterization data for *N*-arylamines

***N*-phenylaniline:** Mp 53 °C. ¹H NMR (300 MHz, CDCl₃): δ(ppm) = 7.33–7.22 (m, 4H), 7.12–7.10 (m, 4H), 6.93–6.89 (m, 2H), 5.69 (s, 1H); ¹³C NMR (100 MHz, CDCl₃): δ(ppm) = 143.3, 128.9, 121.2, 117.3.

***N*-(4-methylphenyl)aniline:** Mp 82 °C. ¹H NMR (300 MHz, CDCl₃): δ(ppm) = 7.17–7.15 (m, 2H), 7.03–7.01 (m, 2H), 6.95–6.92 (m, 4H), 6.83–6.79 (m, 1H), 5.53 (s, 1H), 2.23 (s, 3H); ¹³C NMR (100 MHz, CDCl₃): δ(ppm) = 130.9, 129.8, 129.7, 129.3, 122.7, 120.3, 118.9, 116.9, 20.7.

***N*-(2-methoxyphenyl)aniline:** Oil. ¹H NMR (300 MHz, CDCl₃): δ(ppm) = 7.33–7.30 (m, 3H), 7.17 (d, J = 8 Hz, 2H), 6.98–9.85 (m, 4H), 6.16 (s, 1H), 3.91 (s, 3H); ¹³C NMR (100 MHz, CDCl₃): δ(ppm) = 129.3, 128.8, 121.13, 120.8, 119.9, 118.6, 114.6, 110.5, 55.6.

***N*-(4-methoxyphenyl)aniline:** Mp 103 °C. ¹H NMR (300 MHz, CDCl₃): δ(ppm) = 7.17–7.12 (m, 2H), 7.03–6.99 (m, 2H), 6.86–6.74 (m, 5H), 3.81 (s, 3H); ¹³C NMR (100 MHz, CDCl₃): δ(ppm) = 153.5, 145.7, 135.7, 129.1, 122.4, 119.6, 115.6, 115.1, 55.3.

***N*-(3-methoxyphenyl)aniline:** Oil. ¹H NMR (300 MHz, CDCl₃): δ(ppm) = 7.32–7.28 (m, 2H), 7.22–7.19 (m, 1H), 7.12 (d, 2H), 6.97 (t, 1H), 6.69–6.66 (m, 2H), 6.52–6.50 (m, 1H), 5.74 (s, 1H), 3.81 (s, 3H); ¹³C NMR (100 MHz, CDCl₃): δ(ppm) = 160.2, 144.1, 142.3, 129.6, 128.8, 120.8, 117.8, 109.7, 105.6, 102.8, 54.7.

4-Nitro-*N*-phenylaniline: Mp 132 °C. ¹H NMR (300 MHz, CDCl₃): δ(ppm) = 8.15–8.10 (m, 2H), 7.43–7.36 (m, 2H), 7.23–7.14 (m, 3H), 6.97–6.92 (m, 2H), 6.27 (s, 1H). ¹³C NMR (100 MHz, CDCl₃): δ(ppm) = 150.3, 139.5, 139.4, 129.6, 126.2, 124.5, 121.8, 113.6.

***N*-(4-chlorophenyl)aniline:** Mp 72 °C. ¹H NMR (300 MHz, CDCl₃): δ(ppm) = 7.27–7.20 (m, 2H), 7.14 (d, 2H), 6.99–6.97 (m, 2H), 6.92 (d, 2H), 6.88–6.87 (m, 1H); ¹³C NMR (100 MHz, CDCl₃): δ(ppm) = 142.6, 141.9, 132.3, 129.6, 121.3, 118.8, 115.4.

***N*-(Phenyl)imidazole:** Oil. ¹H NMR (300 MHz, CDCl₃): δ(ppm) = 7.87 (s, 1H), 7.50–7.47 (m, 2H), 7.40–7.37 (m, 3H), 7.29 (s, 1H), 7.21 (s, 1H); ¹³C NMR (100 MHz, CDCl₃): δ(ppm) = 137.47, 135.76, 130.46, 130.06, 127.70, 121.66, 118.45, 107.38.

***N*-Phenylpyrrole:** Mp 62 °C. ¹H NMR (300 MHz, CDCl₃): δ(ppm) = 7.73 (d, 2H), 7.46–7.26 (m, 3H), 7.14–7.11 (m, 2H), 6.38–6.37 (m, 2H); ¹³C NMR (100 MHz, CDCl₃): δ(ppm) = 137.6, 130.4, 129.7, 127.6, 125.7, 120.7, 119.5, 110.4.

4. Conclusions

In summary, an efficient, simple, and cost-effective method for the preparation of Cu-rGO was developed via a one-step electrodeposition method without using toxic reducing agents or volatile solvents. The Cu-rGO was characterized by IR, TGA, XRD, and FE-SEM analyses. The catalyst was successfully utilized for the Ullmann-type *N*-arylation reaction of arylhalides with various amines. Good to high products yields were obtained and the catalyst was easily recoverable and reusable with a negligible reduction in catalytic activity. The most prominent properties of this catalytic system are: the implement of zero-valent copper-based catalyst, which was determined to be inexpensive, air-stable, ligand-free, and effective for Ullmann C–N coupling; and the heterogeneity of the process, which has crucial advantages such as easy separation of products, recyclability and high stability of catalysts.

Conflict of interest

The author has no conflicts of interest to declare.

References

- [1] Devambatla, R. K. V.; Namjoshi, O. A.; Choudhary, S.; Hamel, E.; Shaffer, C. V.; Rohena, C. C.; Mooberry, S. L.; Gangjee, A. Design, Synthesis, and Preclinical Evaluation of 4-Substituted-5-methyl-furo[2,3-d]pyrimidines as Microtubule Targeting Agents That Are Effective against Multidrug Resistant Cancer Cells. *J. Med. Chem.* **2016**, *59*, 5752–5765. <https://doi.org/10.1021/acs.jmedchem.6b00237>.
- [2] Zhang, P.; Yuan, J.; Li, H.; Liu, X.; Xu, X.; Antonietti, M.; Wang, Y. Mesoporous Nitrogen-Doped Carbon for Copper-Mediated Ullmann-Type C-O/N/S Cross-Coupling Reactions. *RSC Adv.* **2013**, *3*, 1890–1895. <https://doi.org/10.1039/C2RA22559J>.
- [3] Senra, J. D.; Aguiar, L. C. S.; Simas, A. B. C. ChemInform Abstract: Recent Progress in Transition Metal Catalyzed C-N Cross-Couplings: Emerging Approaches Towards Sustainability. *Chem. Inform.* **2011**, *42*. <https://doi.org/10.1002/chin.201134221>.
- [4] Jammi, S.; Sakthivel, S.; Rout, L.; Mukherjee, T.; Mandal, S.; Mitra, R.; Saha, P.; Punniyamurthy, T. CuO Nanoparticles Catalyzed C-N, C-O, and C-S Cross-Coupling Reactions: Scope and Mechanism. *J. Org. Chem.* **2009**, *74*, 1971–1976. <https://doi.org/10.1021/jo8024253>.
- [5] Zhou, F.; Guo, J.; Liu, J.; Ding, K.; Yu, S.; Cai, Q. Copper-Catalyzed Desymmetric Intramolecular Ullmann C-N Coupling: An Enantioselective Preparation of Indolines. *J. Am. Chem. Soc.* **2012**, *134*, 14326–14329. <https://doi.org/10.1021/ja306631z>.
- [6] Ikawa, T.; Barder, T. E.; Biscoe, M. R.; Buchwald, S. L. Pd-Catalyzed Amidations of Aryl Chlorides Using Monodentate Biaryl Phosphine Ligands: A Kinetic, Computational, and Synthetic Investigation. *J. Am. Chem. Soc.* **2007**, *129*, 13001–13007. <https://doi.org/10.1021/ja0717414>.
- [7] Dai, Q.; Gao, W.; Liu, D.; Kapes, L. M.; Zhang, X. Triazole-Based Monophosphine Ligands for Palladium-Catalyzed Cross-Coupling Reactions of Aryl Chlorides. *J. Org. Chem.* **2006**, *71*, 3928–3934. <https://doi.org/10.1021/jo060321e>.
- [8] Ali, M. H.; Buchwald, S. L. An Improved Method for the Palladium-Catalyzed Amination of Aryl Iodides. *J. Org. Chem.* **2001**, *66*, 2560–2565. <https://doi.org/10.1021/jo0008486>.
- [9] Huang, X.; Anderson, K. W.; Zim, D.; Jiang, L.; Klapars, A.; Buchwald, S. L. Expanding Pd-Catalyzed C-N Bond-Forming Processes: The First Amidation of Aryl Sulfonates, Aqueous Amination, and Complementarity with Cu-Catalyzed Reactions. *J. Am. Chem. Soc.* **2003**, *125*, 6653–6655. <https://doi.org/10.1021/ja035483w>.
- [10] Gajare, A. S.; Toyota, K.; Yoshifuji, M.; Ozawa, F. Solvent Free Amination Reactions of Aryl Bromides at Room Temperature Catalyzed by a (π -Allyl)palladium Complex Bearing a Diphosphinidene-cyclobutene Ligand. *J. Org. Chem.* **2004**, *69*, 6504–6506. <https://doi.org/10.1021/jo049087n>.
- [11] Rout, L.; Jammi, S.; Punniyamurthy, T. Novel CuO Nanoparticle Catalyzed C-N Cross Coupling of Amines with Iodobenzene. *Org. Lett.* **2007**, *9*, 3397–3399. <https://doi.org/10.1021/ol0713887>.
- [12] Shafir, A.; Buchwald, S. L. Highly Selective Room-Temperature Copper-Catalyzed C-N Coupling Reactions. *J. Am. Chem. Soc.* **2006**, *128*, 8742–8743. <https://doi.org/10.1021/ja063063b>.
- [13] Yang, M.; Liu, F. An Ullmann Coupling of Aryl Iodides and Amines Using an Air-Stable Diazaphospholane Ligand. *J. Org. Chem.* **2007**, *72*, 8969–8971. <https://doi.org/10.1021/jo0712291>.
- [14] Shafir, A.; Lichtor, P. A.; Buchwald, S. L. N-versus O-Arylation of Aminoalcohols: Orthogonal Selectivity in Copper-Based Catalysts. *J. Am. Chem. Soc.* **2007**, *129*, 3490–3491. <https://doi.org/10.1021/ja068926f>.
- [15] Kwong, F. Y.; Buchwald, S. L. Mild and Efficient Copper-Catalyzed Amination of Aryl Bromides with Primary Alkylamines. *Org. Lett.* **2003**, *5*, 793–796. <https://doi.org/10.1021/ol0273396>.
- [16] Rao, H.; Jin, Y.; Fu, H.; Jiang, Y.; Zhao, Y. A Versatile and Efficient Ligand for Copper-Catalyzed Formation of C-N, C-O, and P-C Bonds: Pyrrolidine-2-Phosphonic Acid Phenyl Monoester. *Chem. Eur. J.* **2006**, *12*, 3636–3646. <https://doi.org/10.1002/chem.200501473>.
- [17] Zhang, H.; Cai, Q.; Ma, D. Amino Acid Promoted CuI-Catalyzed C-N Bond Formation between Aryl Halides and Amines or N-Containing Heterocycles. *J. Org. Chem.* **2005**, *70*, 5164–5173. <https://doi.org/10.1021/jo0504464>.
- [18] Mitrofanov, A. Y.; Murashkina, A. V.; Martín-García, I.; Alonso, F.; Beletskaya, I. P. Formation of C-C, C-S and C-N Bonds Catalysed by Supported Copper Nanoparticles. *Catal. Sci. Technol.* **2017**, *7*, 4401–4412. <https://doi.org/10.1039/C7CY01343D>.
- [19] Li, H.; Bai, J.; Wang, J.; Li, C. A Facile Method to Fabricate CuO Supported on Nanofibers as Efficient Catalyst using N-Arylation Reactions. *Mol. Catal.* **2017**, *431*, 49–56. <https://doi.org/10.1016/j.mcat.2017.01.005>.

- [20] Ma, D.; Cai, Q.; Zhang, H. Mild Method for Ullmann Coupling Reaction of Amines and Aryl Halides. *Org. Lett.* **2003**, *5*, 2453–2455. <https://doi.org/10.1021/ol0346584>.
- [21] Garnier, T.; Danel, M.; Magné, V.; Pujol, A.; Bénétteau, V.; Pale, P.; Chassaing, S. Copper(I)-USY as a Ligand-Free and Recyclable Catalyst for Ullmann-Type O-, N-, S-, and C-Arylation Reactions: Scope and Application to Total Synthesis. *J. Org. Chem.* **2018**, *83*, 6408–6422. <https://doi.org/10.1021/acs.joc.8b00620>.
- [22] Gawande, M. B.; Goswami, A.; Felpin, F.-X.; Asefa, T.; Huang, X.; Silva, R.; Zou, X.; Zboril, R.; Varma, R. S. Cu and Cu-Based Nanoparticles: Synthesis and Applications in Catalysis. *Chem. Rev.* **2016**, *116*, 3722–3811. <https://doi.org/10.1021/acs.chemrev.5b00482>.
- [23] Mondal, J.; Biswas, A.; Chiba, S.; Zhao, Y. CuO Nanoparticles Deposited on Nanoporous Polymers: A Recyclable Heterogeneous Nanocatalyst for Ullmann Coupling of Aryl Halides with Amines in Water. *Sci. Rep.* **2015**, *5*, 8294. <https://doi.org/10.1038/srep08294>.
- [24] Reddy, P. L.; Arundhati, R.; Rawat, D. S. Cu(0)/Al₂O₃/SiO₂ NPs: An Efficient Reusable Catalyst for the Cross Coupling Reactions of Aryl Chlorides with Amines and Anilines. *RSC Adv.* **2015**, *5*, 92121–92127. <https://doi.org/10.1039/C5RA19337K>.
- [25] Julkapli, N. M.; Bagheri, S. Graphene Supported Heterogeneous Catalysts: An Overview. *Int. J. Hydrog. Energy* **2015**, *40*, 948–979. <https://doi.org/10.1016/j.ijhydene.2014.10.129>.
- [26] Yan, Y.; Shin, W. I.; Chen, H.; Lee, S.-M.; Manickam, S.; Hanson, S.; Zhao, H.; Lester, E.; Wu, T.; Pang, C. H. A Recent Trend: Application of Graphene in Catalysis. *Carbon Lett.* **2021**, *31*, 177–199. <https://doi.org/10.1007/s42823-020-00200-7>.
- [27] Zhu, J.; Ding, X.; Li, D.; Dou, M.; Lu, M.; Li, Y.; Luo, F. Graphene Oxide-Supported Catalyst with Thermoresponsive Smart Surface for Selective Hydrogenation of Cinnamaldehyde. *ACS Appl. Mater. Interfaces* **2019**, *11*, 16443–16451. <https://doi.org/10.1021/acsami.8b19594>.
- [28] Jafaryan, A.; Sadjadi, S.; Gharib, A.; Ahmadi, S. J. Optimization of Cadmium Adsorption from Aqueous Solutions by Functionalized Graphene and the Reversible Magnetic Recovery of the Adsorbent Using Response Surface Methodology. *Appl. Organomet. Chem.* **2019**, *33*, e5085. <https://doi.org/10.1002/aoc.5085>.
- [29] Mondal, P.; Sinha, A.; Salam, N.; Roy, A. S.; Jana, N. R.; Islam, S. M. Enhanced Catalytic Performance by Copper Nanoparticle-Graphene Based Composite. *RSC Adv.* **2013**, *3*, 5615–5623. <https://doi.org/10.1039/C3RA23280H>.
- [30] Fakhri, P.; Jaleh, B.; Nasrollahzadeh, M. Synthesis and Characterization of Copper Nanoparticles Supported on Reduced Graphene Oxide as a Highly Active and Recyclable Catalyst for the Synthesis of Formamides and Primary Amines. *J. Mol. Catal. A Chem.* **2014**, *383–384*, 17–22. <https://doi.org/10.1016/j.molcata.2013.10.027>.
- [31] Hussain, N.; Gogoi, P.; Azhaganand, V. K.; Shelke, M. V.; Das, M. R. Green Synthesis of Stable Cu(0) Nanoparticles onto Reduced Graphene Oxide Nanosheets: A Reusable Catalyst for the Synthesis of Symmetrical Biaryls from Arylboronic Acids under Base-Free Conditions. *Catal. Sci. Technol.* **2015**, *5*, 1251–1260. <https://doi.org/10.1039/C4CY01229A>.

Supplementary materials

Materials and instruments

All reagents used in this work were of analytical grade or with highest quality and were obtained from Merck (Germany). All solvents including *N,N*-dimethylmethanamide (DMF, 99.8%), dimethyl sulfoxide (DMSO, 99.9%), *N*-methyl-2-pyrrolidone (NMP, 99.0%), acetonitrile (99.5%), toluene (99.5%), and 1,4-dioxane (99.0%) were supplied by Merck (Germany).

All electrochemical tests were carried out by using a potentiostat–galvanostat model PGSTAT302 (from Autolab, Netherlands). Fourier Transformed Infrared (FT-IR) spectra of the samples were collected with a Bruker VECTOR 22 spectrometer (Bruker Optik GmbH, Ettlingen, Germany). Microscopic observation of the bare, rGO- and Cu-rGO-modified electrode was also carried out using a field emission scanning electron microscope (FESEM, ZEISS, Germany). A Philips PW 1800 (USA) diffractometer with a Cu-K α (1.5418 Å) radiation source was used for XRD analysis. Raman spectra were recorded using Bruker Senterra (Germany) using 785 nm laser. Thermogravimetric analysis (TGA) measurements were

recorded on a (TG-DTA, STA 1500, UK) Thermogravimetric. ^1H NMR (300 MHz) and ^{13}C NMR (100 MHz) spectra were recorded on a VARIAN-INOVA (USA) instrument in CDCl_3 as a solvent.

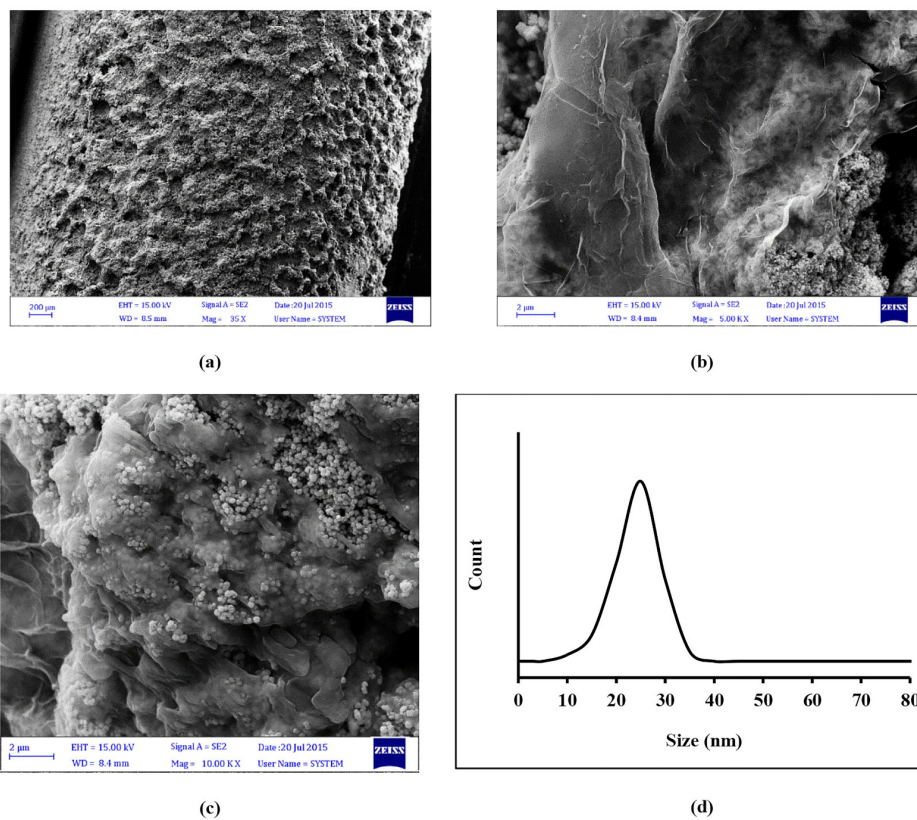


Figure S1. FE-SEM images of (a) bare and (b) rGO- and (c) Cu-rGO-modified electrode; (d) particle size distribution

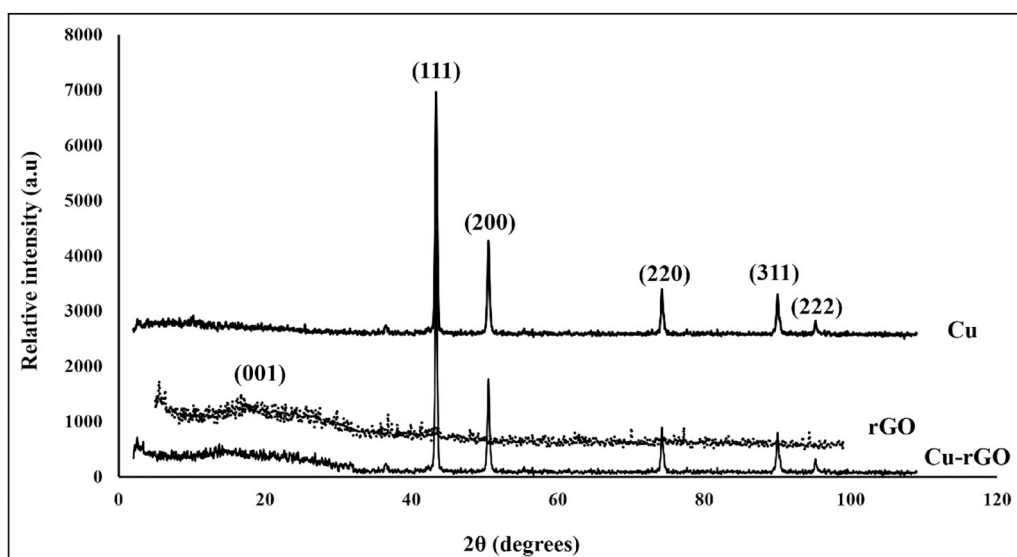


Figure S2. XRD spectra of Cu, rGO, and Cu-rGO

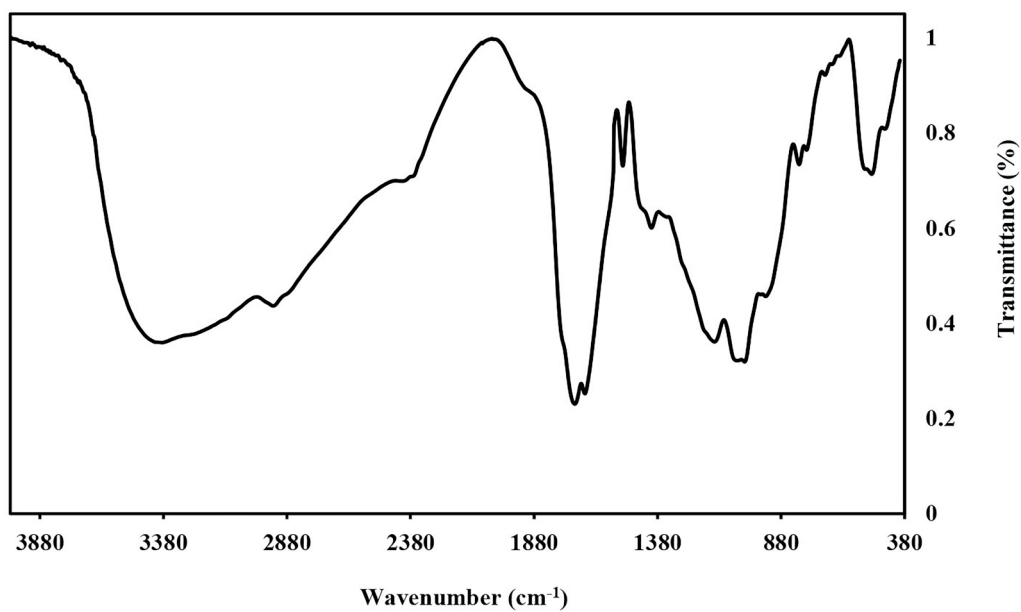


Figure S3. FT-IR spectrum of Cu-rGO

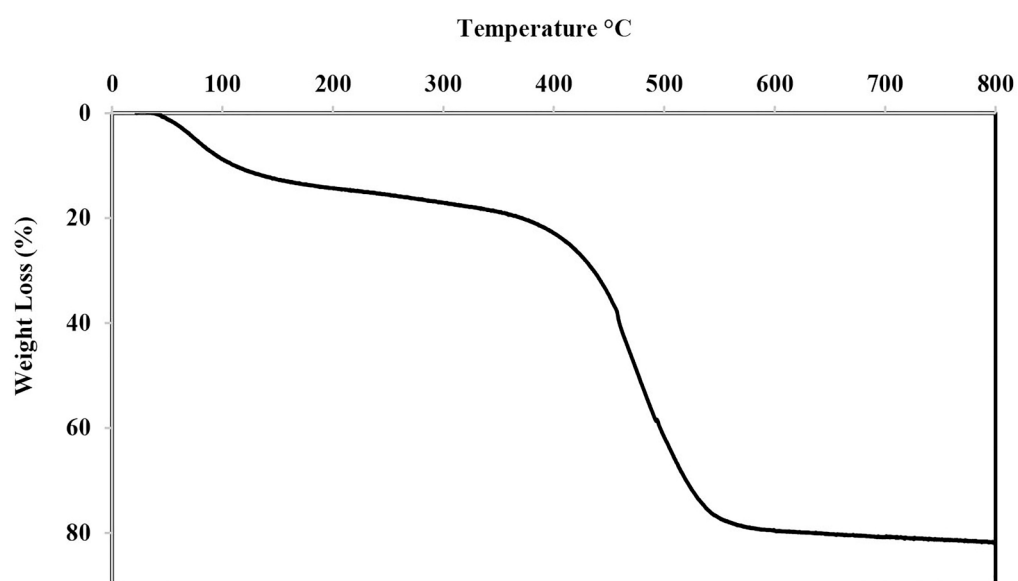


Figure S4. TGA of Cu-rGO